



# Increased sarcolemmal $\text{Na}^+/\text{H}^+$ exchange activity in hypertrophied myocytes from dogs with chronic atrioventricular block

Marcel M. G. J. van Borren<sup>1</sup>, Marc A. Vos<sup>2</sup>, Marien J. C. Houtman<sup>2</sup>, Gudrun Antoons<sup>2</sup> and Jan H. Ravestloot<sup>1\*</sup>

<sup>1</sup> Heart Failure Research Center, Academic Medical Center, University of Amsterdam, Netherlands

<sup>2</sup> Department of Medical Physiology, Division Heart and Lungs, University Medical Center Utrecht, Netherlands

## Edited by:

Mark O. Bevenssee, University of Alabama at Birmingham, USA

## Reviewed by:

Ignacio Gimenez, Aragon's Health Sciences Institute, Spain  
John Cuppoletti, University of Cincinnati, USA

## \*Correspondence:

Jan H. Ravestloot, Department of Anatomy, Embryology, and Physiology, University of Amsterdam, Academic Medical Center, Meibergdreef 15, 1105 AZ, Amsterdam, Netherlands  
e-mail: j.h.ravestloot@amc.uva.nl

Dogs with compensated biventricular hypertrophy due to chronic atrioventricular block (cAVB), are more susceptible to develop drug-induced Torsade-de-Pointes arrhythmias and sudden cardiac death. It has been suggested that the increased  $\text{Na}^+$  influx in hypertrophied cAVB ventricular myocytes contribute to these lethal arrhythmias. The increased  $\text{Na}^+$  influx was not mediated by  $\text{Na}^+$  channels, in fact the  $\text{Na}^+$  current proved reduced in cAVB myocytes. Here we tested the hypothesis that increased activity of the  $\text{Na}^+/\text{H}^+$  exchanger type 1 (NHE-1), commonly observed in hypertrophic hearts, causes the elevated  $\text{Na}^+$  influx. Cardiac acid-base transport was studied with a pH-sensitive fluorescent dye in ventricular myocytes isolated from control and hypertrophied cAVB hearts; the  $\text{H}^+$  equivalent flux through NHE-1,  $\text{Na}^+/\text{HCO}_3^-$  cotransport (NBC),  $\text{Cl}^-/\text{OH}^-$  exchange (CHE), and  $\text{Cl}^-/\text{HCO}_3^-$  exchange (AE) were determined and normalized per liter cell water and corrected for surface-to-volume ratio. In cAVB, sarcolemmal NHE-1 flux was increased by  $65 \pm 6.3\%$  in the pH<sub>i</sub> interval 6.3–7.2 and NBC, AE, and CHE fluxes remained unchanged. Accordingly, at steady-state intracellular pH the total sarcolemmal  $\text{Na}^+$  influx by NHE-1 + NBC increased from  $8.5 \pm 1.5 \text{ amol}/\mu\text{m}^2/\text{min}$  in normal myocytes to  $15 \pm 2.4 \text{ amol}/\mu\text{m}^2/\text{min}$  in hypertrophied cAVB myocytes. We conclude that compensated cardiac hypertrophy in cAVB dogs is accompanied with an increased sarcolemmal NHE-1 activity. This in conjunction with unchanged activity of the other acid-base transporters will raise the intracellular  $\text{Na}^+$  in hypertrophied cAVB myocytes.

**Keywords:** NHE-1, NBC, AE, CHE, compensated cardiac hypertrophy

## INTRODUCTION

Patients with left ventricular hypertrophy are at a higher risk to develop ventricular arrhythmias and sudden cardiac death (Bikkina et al., 1993; Oikarinen et al., 2001). This observation has been confirmed in various animal models with cardiac hypertrophy (Tomaselli and Marban, 1999), including dogs with chronic complete atrioventricular block (cAVB). The cAVB dog has compensated biventricular hypertrophy and a high susceptibility for drug-induced Torsade-de-Pointes arrhythmias (Vos et al., 1998) and sudden cardiac death (van Opstal et al., 2001). These potential lethal arrhythmias have been related to increased spatial (Verduyn et al., 1997) and temporal dispersion (Thomsen et al., 2004) of repolarization (Volders et al., 1999; Antoons et al., 2007).

An important factor that potentially contributes to action potential (AP) changes is the elevated intracellular  $\text{Na}^+$  ( $\text{Na}_i^+$ ) in hypertrophied cAVB ventricular myocytes (Verdonck et al., 2003). High  $\text{Na}_i^+$  is also reported in human hypertrophied myocardium (Gray et al., 2001). This condition reduces  $I_{\text{NCX}}$  inward current during the AP plateau phase thereby limiting AP duration lengthening. When  $\text{Na}_i^+$  is high enough it may even promote NCX-mediated  $\text{Ca}^{2+}$  loading. Indeed, an increase  $\text{Ca}^{2+}$  influx through NCX was observed in cAVB (Sipido et al., 2000). The

high  $\text{Na}_i^+$  in hypertrophied cAVB myocytes has been attributed to an increased  $\text{Na}^+$  influx rather than impaired  $\text{Na}^+$  extrusion through the  $\text{Na}^+/\text{K}^+$  pump (Verdonck et al., 2003). Recent studies indicate that the  $I_{\text{Na}}$  current (peak and late) is decreased and cannot underlie the increased  $\text{Na}^+$  influx in hypertrophied cAVB myocytes (Antoons et al., 2008).

A possible pathway for increased  $\text{Na}^+$  influx in hypertrophied myocardium is the  $\text{Na}^+/\text{H}^+$  exchanger (NHE-1). The activity of NHE-1 is increased in a number of cardiovascular diseases and has been shown to be the major cause for the increased  $\text{Na}_i^+$  concentration commonly observed in the hypertrophied failing hearts (Baartscheer, 2006; Bers et al., 2006). Inhibition of NHE-1 not only lowers  $\text{Na}_i^+$  but also prevents cellular hypertrophy, ionic remodeling, delayed after depolarizations and ultimately the development of heart failure (Baartscheer et al., 2005). Although less-well studied and species dependent, the  $\text{Na}^+/\text{HCO}_3^-$  cotransporter (NBC) is another potential pathway for increased  $\text{Na}^+$  influx (van Borren et al., 2006; Yamamoto et al., 2007). In addition, the extent of  $\text{Na}_i^+$  loading by NHE-1 and NBC largely depends on the supply of acid by the  $\text{Cl}^-$ -dependent acid loaders such as, the  $\text{Cl}^-/\text{OH}^-$  exchanger (CHE) and  $\text{Cl}^-/\text{HCO}_3^-$  exchanger (AE) (Chiappe de Cingolani et al., 2001; van Borren

et al., 2006). However, as yet there is no literature on the identity and characteristics of the cardiac acid-base transporters in dog.

In this study we first confirm the presence of NHE-1, NBC, AE, and CHE in dog ventricular myocytes before we tested the hypothesis that increased sarcolemmal NHE-1 activity underlies the elevated  $\text{Na}^+$  influx in cAVB dogs with compensated biventricular hypertrophy. Here we report that dog ventricular myocytes exhibit NHE-1, NBC, AE, and CHE and that compensated cardiac hypertrophy in cAVB dogs is accompanied with an increased sarcolemmal NHE-1 activity. This together with unchanged sarcolemmal NBC, AE, and CHE activities will raise intracellular  $\text{Na}^+$  concentrations without significant consequences for the resting  $\text{pH}_i$ .

## MATERIALS AND METHODS

Animal handling was performed in accordance with the “European Directive for the Protection of Vertebrate Animals used for Experimental and Scientific Purpose, European Community Directive 86/609/CEE” and under the regulations of “The Committee for Experiments on Animals” of the University of Utrecht, The Netherlands. All research was performed in accordance with the American Physiological Society’s “Guiding Principles in the Care and Use of Animals.”

### ANIMAL MODEL AND CELL ISOLATION

Total atrioventricular (AV) block (AVB) was created in adult dogs (Marshall, USA) of either sex ( $N = 6$ ) by radiofrequency ablation of the AV node as previously described (Schoenmakers et al., 2003). At the time of sacrifice, AVB duration was  $48 \pm 7$  days and body weight  $24 \pm 1$  kg; normal control animals were weight matched ( $N = 5$ ,  $27 \pm 2$  kg). Normal and chronic AVB (cAVB) dogs received full anesthesia. After premedication (1 ml/5 kg: 10 mg oxycodone HCl, 1 mg acepromazine and 0.5 mg atropine, i.m.), sodium pentobarbital (20 mg/kg i.v.) was given. Dogs were artificially ventilated with a mixture of oxygen, nitrous oxide (40:60%), and halothane (0.5–1% vapor concentration). Upon thoracotomy, heparin was administered i.v. The hearts were quickly excised and washed in cold cardioplegic solution. Heart weight/body weight was significantly larger in cAVB dogs ( $12.1 \pm 0.4$  g/kg, vs.  $8.6 \pm 0.3$  g/kg in controls,  $P < 0.05$ ). Single myocytes were enzymatically isolated from the midmyocardial layer of the left and right ventricular free wall, as previously described (Volders et al., 1999).

### SOLUTIONS

Tyrodé’s solution consisted of (mM) 140 NaCl, 5.4 KCl, 1.8  $\text{CaCl}_2$ , 1.0  $\text{MgCl}_2$ , and 5.5 glucose at pH 7.4 ( $37^\circ\text{C}$ ). The normal variant was buffered with 5.0 mM HEPES. In the  $\text{CO}_2/\text{HCO}_3^-$ -buffered variant, 22.4 mM NaCl was replaced by  $\text{NaHCO}_3$  and the saline was gassed with 5%  $\text{CO}_2$  balanced with 95% air. For ammonium prepulses, 20 mM NaCl was replaced by  $\text{NH}_4\text{Cl}$ . For acetate prepulses, 40 or 80 mM NaCl was replaced by NaAcetate (NaAc). In  $\text{Na}^+$ -free Tyrodé’s solutions,  $\text{Na}^+$  was replaced by *N*-methyl-D-glucammonium ( $\text{NMDG}^+$ ) and  $\text{Ca}^{2+}$  was omitted to prevent  $\text{Ca}^{2+}$  loading via reverse mode NCX. In  $\text{Cl}^-$ -free Tyrodé’s solutions  $\text{Cl}^-$  was replaced by gluconate. All salts were purchased from Merck (Darmstadt, Germany). The  $\text{Na}^+/\text{H}^+$  exchanger

inhibitor cariporide was kindly provided by Dr. Pünter (Aventis, Germany). Cariporide was prepared as 1000 $\times$  stock in water.

### INTRACELLULAR $\text{H}^+$ MEASUREMENTS

Myocytes were loaded with the fluorescent pH indicator carboxy-seminaphthorhodafluor-1 (SNARF, Molecular Probes) by exposing them for 10 min to 10  $\mu\text{M}$  of the acetoxymethyl ester at  $35^\circ\text{C}$ . The inverted microscope was equipped with an apparatus for epi-illumination. Dye-loaded myocytes were excited with light of wavelength of 515 nm for 50 ms once every 3 s (75 W Xenon arc lamp). Intensities of the emitted light at wavelengths of 580 ( $I_{580}$ ) and 640 nm ( $I_{640}$ ) were recorded by two photomultiplier tubes. A rectangular adjustable slit ensured negligible background fluorescence levels. The  $I_{580}/I_{640}$  ratio was calibrated by a series of precisely set pH solutions that contained 140 mM  $\text{K}^+$  instead of  $\text{Na}^+$  and 10  $\mu\text{M}$  nigericin (Sigma) (van Borren et al., 2004).

### COMPUTATION OF CYTOPLASMIC $\text{H}^+$ EQUIVALENT FLUX ( $J_{\text{H}^+}^+$ ) PER LITER CELL WATER

Intrinsic buffering power ( $\beta_{\text{int}}$ ) was determined in left and right ventricular myocytes from normal and cAVB dogs. We used the stepwise reduction in  $\text{NH}_3/\text{NH}_4^+$  technique as previously described by van Borren et al. (2004). In short, myocytes were exposed to series of nominally  $\text{Na}^+$  and  $\text{Ca}^{2+}$  free (replaced with *N*-methyl-D-glucammonium ions), HEPES buffered (pH 7.4) Tyrodé’s solutions containing decreasing amounts of  $\text{NH}_3/\text{NH}_4^+$ . To minimize  $\text{NH}_4^+$  entry via  $\text{K}^+$  channels, 2.0 mM  $\text{BaCl}_2$  was added, whereas addition of 1.0 mM  $\text{CdCl}_2$  prevented  $\text{Ba}^{2+}$  influx through L-type  $\text{Ca}^{2+}$  channels.  $\beta_{\text{int}}$  was calculated as  $-\Delta[\text{acid}]_i/\Delta\text{pH}_i$  and assigned to the mean of the two  $\text{pH}_i$  values used for its calculation. The  $\text{CO}_2/\text{HCO}_3^-$  buffering power,  $\beta_{\text{CO}_2}$ , was computed according to:  $\beta_{\text{CO}_2} = 2.3 \times [\text{HCO}_3^-]_o \times 10^{(\text{pH}_i - \text{pH}_o)}$ , with  $[\text{HCO}_3^-]_o$  representing the extracellular  $\text{HCO}_3^-$  concentration. The total buffering power,  $\beta_{\text{tot}}$ , is defined as the sum of  $\beta_{\text{int}}$  and  $\beta_{\text{CO}_2}$ .

To study the  $\text{H}^+$  equivalent flux ( $J_{\text{H}^+}^+$ ) of the acid-base transporters, we imposed an acute acid load followed by an acute alkaline load on the myocytes and allowed them to recover from both. We fitted exponential functions to the recovering  $\text{pH}_i$  traces. From these functions we computed the time derivatives,  $d\text{pH}_i/dt$ ’s, and multiplied these with the appropriate  $\beta_{\text{int}}$  or  $\beta_{\text{tot}}$  to obtain  $J_{\text{H}^+}^+$ . The first 4 min of the  $\text{pH}_i$  recovery from an alkaline load under  $\text{CO}_2/\text{HCO}_3^-$ -buffered conditions were ignored to exclude out-of-equilibrium effects of the cytoplasmic buffering systems.

### COMPUTATION OF SARCOLEMAL $\text{H}^+$ EQUIVALENT FLUX ( $J_{\text{H}^+}^+$ ) PER UNIT MEMBRANE AREA

The sarcolemmal  $J_{\text{H}^+}^+$  per unit area ( $\text{amol}/\mu\text{m}^2/\text{min}$ ) was computed by dividing the cytoplasmic  $J_{\text{H}^+}^+$  by the surface to volume ratios. Atto (symbol a) is an SI prefix representing  $10^{-18}$ . Cell surface was estimated from the membrane capacitance  $C_m$  using a specific membrane capacitance of  $10 \text{ fF}/\mu\text{m}^2$ .  $C_m$  was recorded with the whole-cell ruptured patch-clamp technique, the Axopatch 200B patch-clamp amplifier (Molecular Devices Corporation, Sunnyvale, CA, USA) and borosilicate glass patch pipettes (2–5 M $\Omega$ ) filled with pipette solution containing

(mM): 130 KCl, 10 NaCl, 0.5 MgCl<sub>2</sub>, 5 MgATP, 10 HEPES; pH 7.2 (5.5 KOH). C<sub>m</sub> of right ventricular cAVB myocytes were significantly increased from 182 ± 10 pF (*n* = 29) to 216 ± 13 pF (*n* = 33) (*P* < 0.05), whereas the increase in C<sub>m</sub> of left ventricular cAVB myocytes did not reach statistical significance, from 174 ± 6 pF (*n* = 44) to 187 ± 5 pF (*n* = 93), respectively. Length of left ventricular cAVB myocytes increased from 193 ± 2 μm (*n* = 197) to 225 ± 4 μm (*n* = 154) (*P* < 0.05) and of right ventricular cAVB myocytes from 200 ± 3 μm (*n* = 183) to 244 ± 6 μm (*n* = 154) (*P* < 0.05). Width of left ventricular cAVB myocytes increased from 27 ± 0.4 μm (*n* = 197) to 33 ± 1 μm (*n* = 154) (*P* < 0.05) and of right ventricular cAVB myocytes from 26 ± 0.4 μm (*n* = 183) to 35 ± 1 μm (*n* = 154) (*P* < 0.05). Cell volume was estimated from the morphologic data, assuming cylindrical cell shapes. The surface-to-volume ratios of left ventricular cAVB myocytes was reduced by 38%, from 0.16 ± 0.01 to 0.10 ± 0.01 μm<sup>-1</sup>, and from 0.17 ± 0.02 to 0.09 ± 0.01 μm<sup>-1</sup>, a decrease of 47%, on the right side. By dividing the cytoplasmic J<sub>H</sub><sup>+</sup> (mM/min) by surface-to-volume ratios we arrived at the sarcolemmal J<sub>H</sub><sup>+</sup> per unit area of cell membrane per minute (amol/μm<sup>2</sup>/min).

## STATISTICS

Results are expressed as mean ± standard error (SE). We conducted statistical analyses (linear regression model with repeated measurements, ANOVA Student's *t*-tests) using SPSS® software. Two sets of data were considered significantly different if the *P*-value of these tests was < 0.05. The capital "N" represents the number of hearts used. Lower case "n" represents the number of cells measured.

## RESULTS

### IDENTIFICATION OF SARCOLEMMAL ACID-BASE TRANSPORTERS IN NORMAL DOG VENTRICULAR MYOCYTES

Before studying the differences between normal and hypertrophied cAVB myocytes, we first identified what types of cardiac acid-base transporters are present. Acid-extruders and acid-loaders were activated by imposing acute acid and alkaline loads on the myocytes. Protocols are illustrated in **Figure 1**. In HEPES-buffered solutions, withdrawal of 20 mM NH<sub>3</sub>/NH<sub>4</sub><sup>+</sup> caused an acid load, the recovery from which was CO<sub>2</sub>/HCO<sub>3</sub><sup>-</sup>-independent, but Na<sup>+</sup>-dependent and sensitive to 10 μM cariporide (**Figure 1A**). These characteristics are typical of NHE, presumably of the NHE-1 isoform. We cannot exclude a small contribution of the cariporide sensitive NHE-2 isoform, when present in dog cardiomyocytes. Withdrawal of 40 mM HAc/Ac<sup>-</sup> caused an alkaline load, the recovery from which was CO<sub>2</sub>/HCO<sub>3</sub><sup>-</sup>- and Na<sup>+</sup>-independent but Cl<sup>-</sup>-dependent (**Figure 1B**). These are hallmarks of the Cl<sup>-</sup>/OH<sup>-</sup> exchanger (CHE).

In CO<sub>2</sub>/HCO<sub>3</sub><sup>-</sup>-buffered solutions, a Na<sup>+</sup>-dependent and cariporide-insensitive acid load recovery was observed (**Figure 1C**). These characteristics are typical of the Na<sup>+</sup>-HCO<sub>3</sub><sup>-</sup> cotransporter (NBC). Recovery from an alkaline load upon withdrawal of 80 mM HAc/Ac<sup>-</sup> was CO<sub>2</sub>/HCO<sub>3</sub><sup>-</sup>-dependent and Cl<sup>-</sup>-dependent but Na<sup>+</sup>-independent (**Figure 1D**). These are the hallmarks of the Cl<sup>-</sup>/HCO<sub>3</sub><sup>-</sup> exchanger (anion exchanger, AE). The recovery from an alkaline load in CO<sub>2</sub>/HCO<sub>3</sub><sup>-</sup>-buffered solutions is presumably mediated by both CHE and AE.

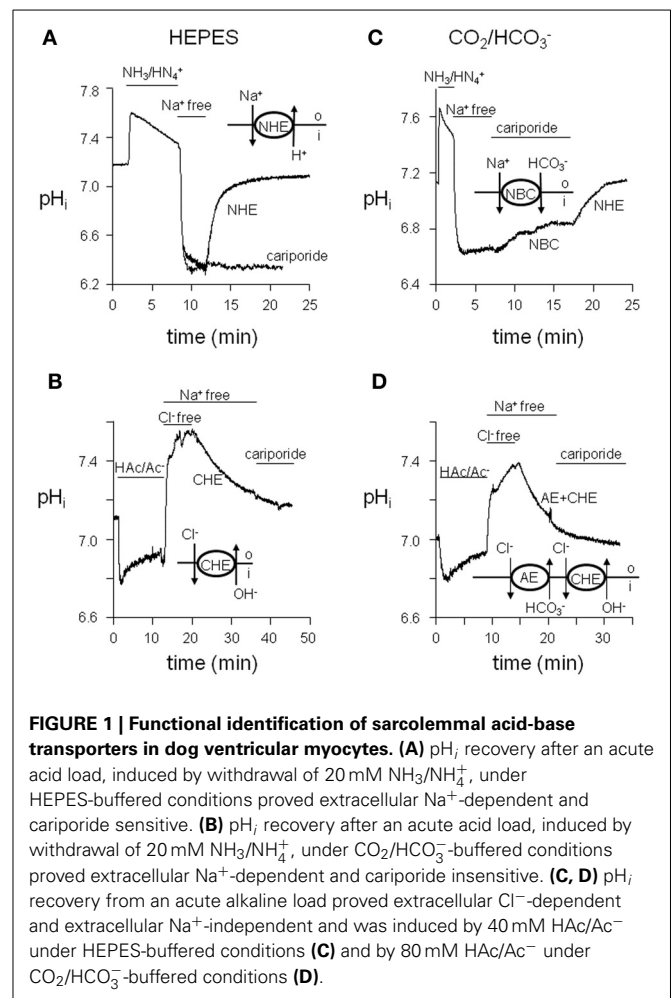


**FIGURE 1 | Functional identification of sarcolemmal acid-base transporters in dog ventricular myocytes. (A)** p<sub>H<sub>i</sub></sub> recovery after an acute acid load, induced by withdrawal of 20 mM NH<sub>3</sub>/NH<sub>4</sub><sup>+</sup>, under HEPES-buffered conditions proved extracellular Na<sup>+</sup>-dependent and cariporide sensitive. **(B)** p<sub>H<sub>i</sub></sub> recovery after an acute alkaline load, induced by withdrawal of 40 mM HAc/Ac<sup>-</sup>, under HEPES-buffered conditions proved extracellular Cl<sup>-</sup>-dependent and Na<sup>+</sup>-independent. **(C, D)** p<sub>H<sub>i</sub></sub> recovery from an acute alkaline load proved extracellular Na<sup>+</sup>-independent and was induced by 80 mM HAc/Ac<sup>-</sup> under CO<sub>2</sub>/HCO<sub>3</sub><sup>-</sup>-buffered conditions **(D)**.

From these data we conclude that dog cardiac myocytes possess the four classical acid-base transporters NHE-1, CHE, NBC, and AE.

### PROTOCOL USED TO STUDY ALL ACID-BASE TRANSPORTERS IN ONE MYOCYTE

To limit the time needed for studying all acid-base transporters, we designed a protocol for measuring NHE-1, NBC, AE, and CHE activity in one myocyte. A typical example is shown in **Figure 2**.

We first imposed an acid-load on a myocyte (NH<sub>3</sub>/NH<sub>4</sub><sup>+</sup> prepulse technique) under HEPES-buffered conditions. The acid-load was quickly alleviated by means of NHE-1 until p<sub>H<sub>i</sub></sub> balanced was reached, the p<sub>H<sub>i</sub></sub> value at which an acid-base transporter is exactly balanced by the opposing J<sub>H</sub><sup>+</sup> flux (dp<sub>H<sub>i</sub></sub>/dt equals 0). The myocyte was then subjected to a mild acid-load by replacing HEPES with 5% CO<sub>2</sub>/22.4 mM HCO<sub>3</sub><sup>-</sup> (pH 7.4) in the presence of 10 μM cariporide to inhibit NHE-1. The only acid-extruder active under these conditions is the HCO<sub>3</sub><sup>-</sup>-dependent NBC. The NBC-mediated recovery was slow and incomplete, and stopped at the near neutral p<sub>H<sub>i</sub></sub> balanced value. Washout of cariporide unblocked NHE-1, which led to further restoration of p<sub>H<sub>i</sub></sub> until the original steady-state p<sub>H<sub>i</sub></sub> value under CO<sub>2</sub>/HCO<sub>3</sub><sup>-</sup>-buffered conditions once again was reached. Thereafter, the myocyte was alkaline

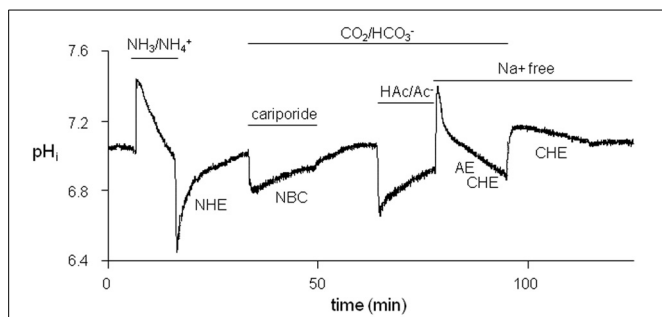


**FIGURE 2 | Typical protocol used to successively examine the four sarcolemmal acid-base transporters in each myocyte.** Firstly, NHE-1 was studied after an acid-load induced by withdrawal of 20 mM  $\text{NH}_4^+/\text{NH}_3$ . Secondly, NBC was studied, while NHE-1 was inhibited by cariporide, following a second weak acid load induced by replacement of a HEPES-buffered Tyrode's solution by a  $\text{CO}_2/\text{HCO}_3^-$ -buffered Tyrode's solution. Thirdly, AE + CHE was studied in a  $\text{Na}^+$ -free  $\text{CO}_2/\text{HCO}_3^-$ -buffered saline solution after an alkaline load was induced by washout of 80 mM  $\text{HAc}/\text{Ac}^-$ . Finally, CHE was studied in  $\text{Na}^+$ -free conditions after an alkaline load was induced by replacing  $\text{CO}_2/\text{HCO}_3^-$ -buffered with HEPES-buffered Tyrode's solutions.

loaded ( $\text{HAc}/\text{Ac}^-$  prepulse technique). The recovery from this load occurred quickly by means of AE and CHE. By choosing  $\text{Na}^+$ -free condition at this stage of the experiment the  $\text{Cl}^-$ -dependent acid-loaders were not opposed by the  $\text{Na}^+$ -dependent acid extruders at neutral  $\text{pH}_i$  values. In this way their  $\text{H}^+$  equivalent flux at the steady-state  $\text{pH}_i$  could be determined. Finally, the myocyte was subjected to second and mild alkaline load (replacing  $\text{CO}_2/\text{HCO}_3^-$  with HEPES). From this alkaline load the myocytes recovered only very slowly by means of CHE and stopped recovering when CHE  $\text{pH}_{i,\text{balanced}}$  value was reached.

### INTRINSIC BUFFERING POWER ( $\beta_{\text{int}}$ ) IN NORMAL AND HYPERTROPHIED cAVB MYOCYTES

To compute cytoplasmic  $\text{H}^+$  equivalent fluxes ( $J_{\text{H}^+}$ ) from  $\text{pH}_i$  recovery rates, we determined the  $\text{pH}_i$ -dependence of the intrinsic buffering power ( $\text{pH}_i$ - $\beta_{\text{int}}$ ) in left and right ventricular myocytes of normal (left  $N = 2$ ;  $n = 7$  and right  $N = 2$ ;  $n = 7$ ) and cAVB (left  $N = 2$ ;  $n = 15$  and right  $N = 2$ ;  $n = 12$ ) dogs. Myocytes exposed to a series of  $\text{NH}_4^+/\text{NH}_3$  (20–2.5 mM) solutions showed a stepwise reduction in  $\text{pH}_i$  (Figure 3A). The  $\text{pH}_i$ - $\beta_{\text{int}}$  relationships did not significantly differ between myocytes isolated from the left and right ventricle, or between normal and cAVB hearts (data not shown). For this reason we pooled all data and calculated the average  $\text{pH}_i$ - $\beta_{\text{int}}$  relationship ( $N = 4$ ;  $n = 41$ ). The averaged  $\text{pH}_i$ - $\beta_{\text{int}}$  relationship was fitted with a polynomial equation (Figure 3B). Cytoplasmic  $J_{\text{H}^+}$  was calculated at 0.05  $\text{pH}_i$  intervals. Next, cytoplasmic  $J_{\text{H}^+}$  were divided by the averaged surface-to-volume ratios and plotted as a function of the corresponding  $\text{pH}_i$  to construct sarcolemmal  $\text{pH}_i$ - $J_{\text{H}^+}$  profiles of NHE-1 ( $\text{pH}_i$ - $J_{\text{NHE-1}}$ ), NBC ( $\text{pH}_i$ - $J_{\text{NBC}}$ ), AE + CHE ( $\text{pH}_i$ - $J_{\text{AE+CHE}}$ ), and CHE ( $\text{pH}_i$ - $J_{\text{CHE}}$ ).

### SARCOLEMAL $\text{pH}_i$ - $J_{\text{H}^+}$ PROFILES IN NORMAL LEFT AND RIGHT VENTRICULAR MYOCYTES

In both left ( $n = 12$ ) and right ( $n = 9$ ) ventricular myocytes from normal dog hearts ( $N = 4$ ) sarcolemmal  $J_{\text{NHE-1}}$  (i) were equally

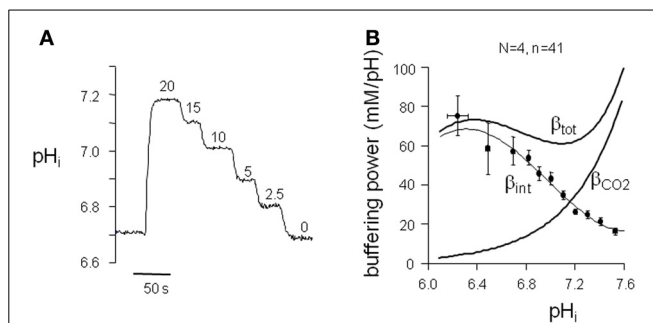


**FIGURE 3 |  $\text{pH}_i$  dependence of buffering power in dog ventricular myocytes.** (A) Typical  $\text{pH}_i$  trace of a protocol to determine the intrinsic buffering power ( $\beta_{\text{int}}$ ) of ventricular myocytes. (B) The  $\beta_{\text{int}}$  values, within a 0.05  $\text{pH}_i$  range, were averaged and plotted against the appropriate  $\text{pH}_i$ ; to construct the  $\text{pH}_i$ - $\beta_{\text{int}}$  relationship. The polynomial fit through the data is used to calculate  $J_{\text{H}^+}$  under HEPES-buffered conditions. For  $J_{\text{H}^+}$  under  $\text{CO}_2/\text{HCO}_3^-$ -buffered conditions the calculated  $\beta_{\text{CO}_2}$  was added to  $\beta_{\text{int}}$  to arrive at  $\beta_{\text{tot}}$ .

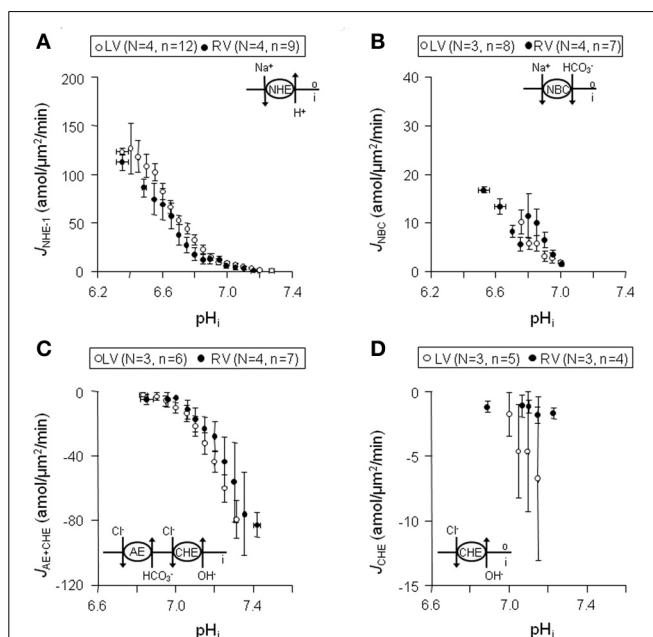


**FIGURE 4 | Sarcolemmal  $J_{\text{H}^+}$  through NHE-1, NBC, CHE + AE, and CHE in normal left and right ventricular myocytes.** Data obtained from left are shown in blank circles, whereas from right are indicated with filled circles. Panels (A–D) illustrates that sarcolemmal  $J_{\text{NHE-1}}$  (A),  $J_{\text{NBC}}$  (B),  $J_{\text{AE+CHE}}$  (C), and  $J_{\text{CHE}}$  (D) are not significantly different throughout the whole  $\text{pH}_i$  range in left compared to right ventricular myocytes.

large at acidic  $\text{pH}_i$  values, (ii) showed a comparable steep  $\text{pH}_i$ -dependency, and (iii) had similar  $\text{pH}_{i,\text{balanced}}$  values (Figure 4A). Likewise, no differences in these three characteristics were found in sarcolemmal  $J_{\text{NBC}}$ , between left ( $N = 3$ ,  $n = 8$ ) and right ( $N = 4$ ,  $n = 7$ ) ventricular myocytes (Figure 4B). Compared to NHE-1, (i) NBC fluxes were 77% smaller, (ii) NBC  $\text{pH}_i$ -dependence was 7-fold less, and (iii) NBC  $\text{pH}_{i,\text{balanced}}$  value was  $\sim 0.2$  pH more acidic. Thus, NHE-1 is the major acid extruder present in the dog myocardium.

The myocytes showed a rapid alkaline load recovery under  $\text{CO}_2/\text{HCO}_3^-$ -buffered conditions. In left ( $N = 3, n = 6$ ) and right ( $N = 4, n = 7$ ) ventricular myocytes sarcolemmal  $J_{\text{AE}+\text{CHE}}$  was (i) equally large at alkaline  $\text{pH}_i$  values, (ii) showed a comparable  $\text{pH}_i$ -dependency, and (iii) had a virtually identical  $\text{pH}_i$ , balanced value of around 6.8 (Figure 4C). Unlike sarcolemmal  $J_{\text{AE}+\text{CHE}}$ , sarcolemmal  $J_{\text{CHE}}$  proved small and only weakly  $\text{pH}_i$  dependent. Again, no differences were observed between left ( $N = 3, n = 5$ ) and right ( $N = 3, n = 4$ ) ventricular myocytes (Figure 4D). Thus, AE is the major acid loader present in the dog myocardium and is largely responsible for alkaline load recoveries under  $\text{CO}_2/\text{HCO}_3^-$ -buffered conditions.

We conclude that no differences exist in sarcolemmal  $\text{pH}_i$ - $J_{\text{H}}^+$  profiles of NHE-1, NBC, AE, and CHE between myocytes from the left and right ventricle.

**SARCOLEMMA  $\text{pH}_i$ - $J_{\text{H}}^+$  PROFILES IN NORMAL AND HYPERTROPHIED cAVB MYOCYTES**

Next, we examined whether the sarcolemmal  $\text{pH}_i$ - $J_{\text{H}}^+$  profiles were changed in hypertrophied cAVB myocytes. Like in normal dog hearts, no differences were observed in the sarcolemmal  $\text{pH}_i$ - $J_{\text{H}}^+$  profiles between left and right hypertrophied ventricular cAVB myocytes (data not shown). For this reason the pooled left and right sarcolemmal  $\text{pH}_i$ - $J_{\text{H}}^+$  profiles of hypertrophied cAVB myocytes were compared to the pooled left and right sarcolemmal  $\text{pH}_i$ - $J_{\text{H}}^+$  profiles of normal myocytes (Figure 5).

In hypertrophied cAVB myocytes the sarcolemmal  $J_{\text{NHE-1}}$  (Figure 5A), (i) was significantly increased at  $\text{pH}_i$  values

more acidic than 7.05 ( $P < 0.05$ ), the increase amounted to  $65 \pm 6.3\%$  in the  $\text{pH}_i$  interval 6.3–7.2, (ii) showed a 75% steeper  $\text{pH}_i$ -dependency,  $-4.4 \pm 2.2 \text{ amol}/\mu\text{m}^2/\text{min}/\text{pH}$  unit ( $n = 25$ ) vs.  $-2.2 \pm 3.4 \text{ amol}/\mu\text{m}^2/\text{min}/\text{pH}$  unit ( $n = 21$ ) ( $P < 0.05$ ), and (iii) identical  $\text{pH}_i$ , balanced values of around 7.3. In contrast, no changes were observed in the sarcolemmal  $\text{pH}_i$ - $J_{\text{NBC}}$  (Figure 5B),  $\text{pH}_i$ - $J_{\text{AE}+\text{CHE}}$  (Figure 5C), and  $\text{pH}_i$ - $J_{\text{CHE}}$  (Figure 5D) profiles between normal myocytes and hypertrophied cAVB myocytes.

From these data we conclude that sarcolemmal  $J_{\text{NHE-1}}$  is increased in hypertrophied cAVB myocytes but otherwise there are no significant differences in sarcolemmal acid-base transport between normal hearts and compensated biventricular hypertrophied hearts.

**SARCOLEMMA  $J_{\text{H}}^+$  AT RESTING  $\text{pH}_i$  IN NORMAL AND HYPERTROPHIED cAVB MYOCYTES**

When metabolic acid-base production is neglected, resting  $\text{pH}_i$  is defined by the balance of acid loading ( $J_{\text{CHE}}$  and/or  $J_{\text{AE}}$ ) and acid extrusion ( $J_{\text{NHE-1}}$  and/or  $J_{\text{NBC}}$ ). As is shown in Figure 6A, neither under HEPES-buffered conditions nor under  $\text{CO}_2/\text{HCO}_3^-$ -buffered conditions the resting  $\text{pH}_i$  of normal and hypertrophied cAVB myocytes differed significantly. However, in both groups the resting  $\text{pH}_i$  was significantly more alkaline under HEPES-buffered conditions as compared to  $\text{CO}_2/\text{HCO}_3^-$ -buffered conditions ( $P < 0.05$ ). This difference indicates that in  $\text{CO}_2/\text{HCO}_3^-$ -buffered solutions the acid loading action of AE

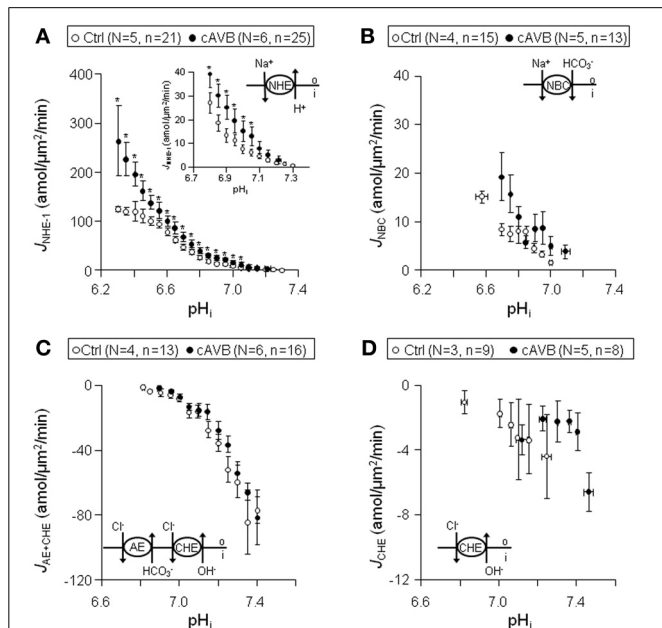


**FIGURE 5 | Sarcolemmal  $J_{\text{H}}^+$  through NHE-1, NBC, CHE + AE, and CHE in normal and hypertrophied cAVB ventricular myocytes.** Pooled data (LV + RV) obtained from normal (open circles) and cAVB myocytes (filled circles). Panels (A–D) illustrates sarcolemmal  $\text{pH}_i$ - $J_{\text{NHE-1}}$  (A),  $\text{pH}_i$ - $J_{\text{NBC}}$  (B),  $\text{pH}_i$ - $J_{\text{AE}+\text{CHE}}$  (C), and  $\text{pH}_i$ - $J_{\text{CHE}}$  (D) profiles. Asterisks “\*” indicate statistical significance.

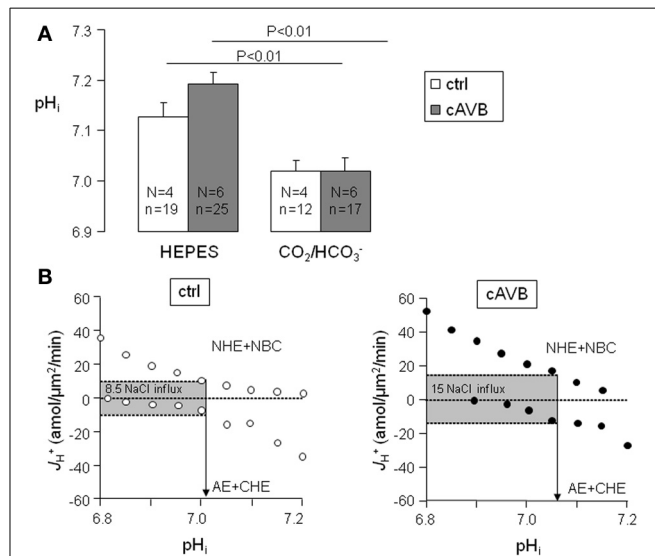


**FIGURE 6 | Balanced cytoplasmic  $J_{\text{H}}^+$  and sarcolemmal  $J_{\text{H}}^+$  at steady-state  $\text{pH}_i$  in normal and cAVB myocytes.** (A) Steady-state  $\text{pH}_i$  values were obtained in normal (open bars) and cAVB (filled bars) myocytes either under HEPES or  $\text{CO}_2/\text{HCO}_3^-$ -buffered conditions. Significant differences ( $P < 0.01$ ), the number of animals (N) and observations (n) are indicated. (B) Total sarcolemmal  $J_{\text{H}}^+$  of the acid extruders and the acid loaders are plotted against their  $\text{pH}_i$  in one graph to visualize their overlap at the steady-state  $\text{pH}_i$ .  $J_{\text{H}}^+$  of the acid extruders and acid loaders are balanced in normal myocytes at  $\text{pH}_i$  7.01 (B, left panel) and in cAVB myocytes at  $\text{pH}_i$  7.07 (B, right panel), causing respectively a sarcolemmal  $J_{\text{H}}^+$  of 8.5 and  $15 \text{ amol}/\mu\text{m}^2/\text{min}$  at these  $\text{pH}_i$  values.

drives  $pH_i$  more acidic. In the process NHE-1 and NBC increase their activity. At the new steady-state  $pH_i$ , acid loading is balanced by acid extrusion, and the cell experiences increased NaCl influx as compared to HEPES-buffered conditions. We estimated the magnitude of the increased sarcolemmal NaCl influx from the sarcolemmal  $pH_i$ - $J_H^+$  profiles of the four acid base transporters (Figure 4). In physiological,  $CO_2/HCO_3^-$ -buffered solutions the sarcolemmal  $J_H^+$ , at the resting  $pH_i$  increased from  $8.5 \pm 1.5$  amol/ $\mu m^2$ /min in normal myocytes (Figure 6B, left panel) to  $15 \pm 2.4$  amol/ $\mu m^2$ /min in hypertrophied cAVB myocytes (Figure 6B, right panel). Thus, the sarcolemmal  $Na^+$  influx in  $CO_2/HCO_3^-$ -buffered solutions at resting  $pH_i$  is increased by 76% in hypertrophied cAVB myocytes.

From these data we conclude that at resting  $pH_i$  there are substantial differences in NaCl loading between normal hearts and compensated biventricular hypertrophied hearts.

## DISCUSSION

### OVERVIEW

We investigated acid-base transport in normal dog hearts, and in hearts from cAVB dogs with compensated hypertrophy. We first identified (Figures 1, 2) and characterized the sarcolemmal acid-base transporters. After determination of the intrinsic cytoplasmic buffering power (Figure 3) we constructed their  $pH_i$ - $J_H^+$  profiles (Figure 4). NHE-1 and AE are the most potent acid extruder and acid loader, respectively, whereas the contribution of NBC and CHE to  $pH_i$  regulation is relatively small (Figure 4). Secondly, neither in normal myocytes nor in hypertrophied cAVB myocytes did we observed left and right differences in acid-base transport (Figure 4). Thirdly, we demonstrated that compensated biventricular hypertrophy is associated with increased sarcolemmal NHE-1 mediated  $H^+$  equivalent fluxes but unchanged NBC, AE, or CHE fluxes (Figures 5, 6). Consequently, at resting  $pH_i$  values, the amount sarcolemmal  $Na^+$  influx is significantly increased in hypertrophied cAVB myocytes (Figure 6).

### ACID-BASE TRANSPORT OF NORMAL DOG VENTRICULAR MYOCYTES

In the past, the role of NHE-1 has been pharmacologically examined in dog hearts with respect to ischemia/reperfusion injury and ischemic preconditioning (Gumina et al., 2000, 2005; Oh et al., 2007), however nothing is known about its activity and  $pH_i$ -sensitivity. In addition, molecular, pharmacological, and functional data on NBC, AE, and CHE in the dog myocardium are completely lacking. To gain insight in what type of acid-base transporters are present in dog ventricular myocytes we used the experimental approach previously published for guinea-pig and rabbit ventricular myocytes (Leem et al., 1999; van Borren et al., 2006). Except for minor quantitative differences there is good agreement between our data and those published for guinea pig and rabbit. In these species CHE contributes for 15–30% to the acid loading rate (Leem and Vaughan-Jones, 1998), whereas we found a contribution of less than 10% in dog ventricular myocytes. The remaining acid-loading capacity can be attributed to AE. It should be noted that in this study we cannot exclude a possible contribution of residual  $Cl^-/HCO_3^-$  exchange during the alkaline-load recovery under HEPES-buffered conditions.

In dog, NHE-1 is responsible for more than 80% to the total acid extrusion capacity. Similar transport rates were found in

rabbit (65%) guinea-pig (Lagadic-Gossmann et al., 1992; Leem et al., 1999), rat (Le Prigent et al., 1997) and sheep purkinje fiber (Dart and Vaughan-Jones, 1992). The other 20% of the acid-extrusion capacity can be attributed to NBC. In this study we did not determine the relative contribution of the different NBC isoforms [electroneutral (NBCn) vs. electrogenic (NBCe)] (Yamamoto et al., 2005). Moreover, the expression levels and molecular identities of the acid-base transporters remain to be determined.

Differences in membrane protein expression levels between left and right ventricular myocardium have been described. For example the current densities of the repolarizing potassium currents, the transient outward potassium current ( $I_{to}$ ) and the delayed rectifier ( $I_{Ks}$ ), are larger in right ventricular myocytes (Volders et al., 1999; Di Diego et al., 2002) and may underlie the consequent shorter AP. Also left-right differences in  $Ca_i^{2+}$  transients and contractions were observed. However, the smaller  $Ca_i^{2+}$  transients and contractions of right ventricular myocytes were not related to differential expression of  $Ca_i^{2+}$  handling proteins but to the shorter APs (Kondo et al., 2006).

In this study we demonstrated that steady-state  $pH_i$  as well as acid-base transport activity of NHE-1, NBC, AE, and CHE do not differ between left and right ventricular myocytes of dogs hearts.

### DECREASED SURFACE-TO-VOLUME RATIO IN HYPERTROPHIED cAVB MYOCYTES

Comparison of membrane transport activities, e.g., acid-base transporters, between cells is only allowed when they exhibit an identical cell surface-to-volume ratio value. It has been shown that these values can differ between species and between developmental stages, but are similar between small and large myocytes from the same healthy hearts (Satoh et al., 1996). During cardiac hypertrophy myocyte shape alterations parallel changes in ventricular anatomy (Gerdes, 2002). Indeed, isolated ventricular myocytes of cAVB dogs with eccentric biventricular hypertrophy increased more in length (13–23%) than in width (4–13%). Irrespective whether cells were assumed cylindrical or brick shaped, the cell volume of hypertrophied cAVB myocytes (74–121%) increased more than the surface area (14–26%). Consequently, surface-to-volume ratio decreased in hypertrophied cAVB myocytes by 38–47%. In modest hypertrophy, cardiomyocytes are able to maintain a normal surface-to-volume ratio by increasing T-tubular surface area disproportionately (Gerdes, 2002). Apparently this is not the case in compensated hypertrophied hearts of dogs with cAVB. Changes in surface-to-volume ratios between normal and hypertrophied myocytes have also been found in rat with cardiac hypertrophy (Yamamoto et al., 2007).

### ACID-BASE TRANSPORT IN HYPERTROPHIED cAVB MYOCYTES

Increased NHE-1 activity is observed in human hypertrophied cardiomyocytes (Yokoyama et al., 2000) and in hypertrophied myocytes from various animal models with hypertension or heart failure (Baartscheer, 2006). For instance in rats with monocrotaline-induced right ventricular failure (Chen et al., 2001), in diabetes type-2 rats (Darmellah et al., 2007) and spontaneous hypertensive rats (SHR) (Cingolani et al., 2003; Ennis et al., 2007) with heart failure, and in pressure and volume

(Baartscheer et al., 2003; van Borren et al., 2006) and rapid pacing (Aker et al., 2004) induced rabbit models of heart failure NHE-1 activity is markedly enhanced. Both post-translational modulation and increased protein expression have been proposed to cause increased NHE-1 activity (Cingolani et al., 2008). In a number of these animal models chronic NHE-1 inhibition prevented (Kusumoto et al., 2001; Sandmann et al., 2001; Baartscheer et al., 2005) or even reversed the development of hypertrophy or heart failure (Camilion de Hurtado et al., 2002; Cingolani et al., 2003; Baartscheer et al., 2008; Baartscheer and van Borren, 2008). Moreover, transgenic mice with arterial hypertension (lacking the natriuretic peptide receptor type A) (Kilic et al., 2005) or heart failure (beta-adrenergic receptor over-expressing in the heart) (Engelhardt et al., 2002) developed cardiac hypertrophy and exhibit increased NHE-1 activity. Also in these transgenic animal models, NHE-1 inhibition prevented the development of cardiac hypertrophy and heart failure. Recently it became clear that increased cardiac NHE-1 activity alone is sufficient to activate hypertrophic  $Ca_i^{2+}$  dependent signaling pathways (Nakamura et al., 2008) and to induce dilated hypertrophic cardiomyopathy (Coccaro et al., 2007; Nakamura et al., 2008). Together, these studies underscore the pivotal role of increased NHE-1 activity in the etiology of hypertrophy and heart failure.

In good agreement with the aforementioned models of cardiac hypertrophy and heart failure, we demonstrated here that also in cAVB dogs with compensated biventricular hypertrophy, sarcolemmal NHE-1 flux is increased. It should be noted that our cAVB dogs are free from heart failure symptoms, hypertension and lack the substantial sustained or progressive increase in the levels of neurohumoral factors (Vos et al., 1998). This suggests that hypertrophy *per se* is associated with increased sarcolemmal NHE-1 activity. Mechanisms underlying increased sarcolemmal NHE-1 activity in compensated hypertrophied hearts require further investigation, but may include increased wall stretch.

AE, NBC, and CHE, have been studied less extensively than NHE-1. An increased cardiac AE exchange activity has been documented in SHR (Chiappe de Cingolani et al., 2001) and rabbits with heart failure (pressure and volume overload) (van Borren et al., 2006). In our model of compensated cardiac hypertrophy, AE proved unchanged. Perhaps hypertension or heart failure is essential for increased AE activity to occur. Contradicting data exist on NBC. In one study NBC activity proved increased in hypertrophied cardiomyocytes from pressure overloaded rats (Yamamoto et al., 2007), whereas in another NBC activity was unchanged in hypertrophied cardiomyocytes from rabbits with heart failure (pressure and volume overload) (van Borren et al., 2006). Here we add that compensated hypertrophy does not increase cardiac NBC activity. Moreover, like in rabbits with heart failure (van Borren et al., 2006) no significant changes in CHE activity was observed in hypertrophied cAVB myocytes.

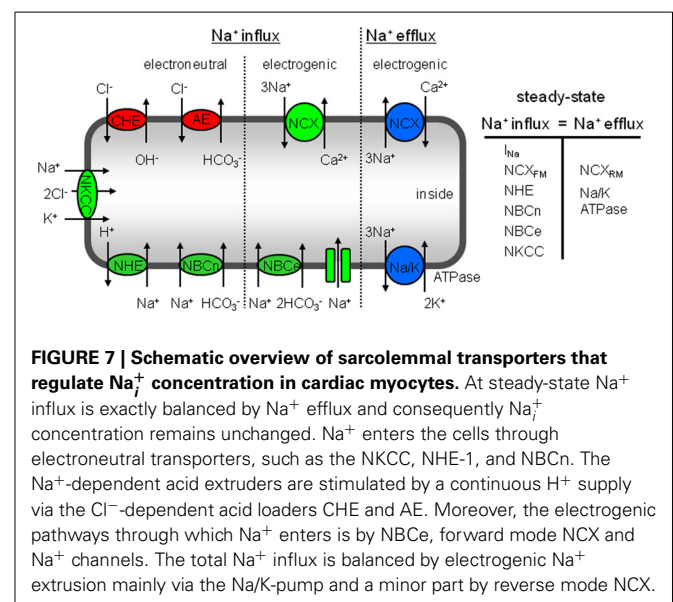
### CARDIAC ACID-BASE TRANSPORT CAN EXPLAIN INCREASED $Na^+$ INFLUX IN HYPERTROPHIED cAVB MYOCYTES

The high  $Na_i^+$  levels observed in hypertrophied cAVB myocytes have been attributed to a reduced affinity of the Na/K pump for  $Na_i^+$  removal and to an increased  $Na^+$  influx (Verdonck et al., 2003). The latter was indirectly derived from Na/K pump

currents, the major pathway for  $Na^+$  efflux that must equal  $Na^+$  influx under steady-state conditions in resting myocytes. A recent study revealed that hypertrophied cAVB myocytes exhibit both a reduced peak and late  $I_{Na}$ , which excludes the sodium channels as a potential source for the enhanced  $Na^+$  influx (Antoons et al., 2008). Our data demonstrate that the balanced sarcolemmal  $J_H^+$  flux ( $J_{NHE-1+NBC}$  and  $J_{CHE+AE}$ ) at steady-state  $pH_i$  (Figure 6) is increased by 76%. The increased sarcolemmal  $Na^+$  influx through balanced acid-base transport needs to be fully compensated by the sarcolemmal Na/K pump. As previously reported by Verdonck et al., the maximal Na/K pump activity (pA/pF, a measure per  $\mu m^2$ ) remains unchanged and the affinity of the Na/K pump for  $Na_i^+$  is reduced (Verdonck et al., 2003). Therefore, in hypertrophied cAVB myocytes the Na/K pump activity can only be sufficiently increased at higher  $Na_i^+$  concentrations. The higher NHE-1-mediated  $Na^+$  influx calculated in this study (76%, Figure 6) closely matches the relative increase of pump current densities in hypertrophied cAVB myocytes (88%) observed by Verdonck et al. (2003). This implies that NHE-1 is the main pathway responsible for increased  $Na^+$  influx. Other influx pathways, such as NCX or Na-K-2Cl cotransporter (NKCC, Figure 7) may have a contribution as well. NCX, however, is an unlikely candidate because elevated  $Na_i^+$  would rather promote the reverse mode and load the cell with  $Ca_i^{2+}$ , in particular in a setting of prolonged APs, as observed in cAVB (Pogwizd et al., 2003). Indeed, increased NCX-mediated  $Ca^{2+}$  loading was observed in hypertrophied cAVB myocytes (Sipido et al., 2000). NKCC may be an additional pathway for increased  $Na^+$  influx in cAVB, as documented previously for heart failure (Andersen et al., 2006). We cannot exclude a small contribution of NHE-2, when present in dog cardiomyocytes, since this transporter is also inhibited at the cariporide concentrations we used to identify NHE-1.

### CONCLUSION

Dogs exhibit four cardiac acid-base transporters, namely NHE-1, NBC, CHE, and AE. Their activities do not differ between left and



right ventricular myocytes. Compensated hypertrophied hearts from cAVB dogs exhibit increased sarcolemmal  $J_{\text{NHE-1}}$  activity that almost fully explains the elevated  $\text{Na}^+$  influx in these hearts. Whether NHE-1 inhibition can prevent drug-induced Torsade-de-Pointes arrhythmias in cAVB dogs will be subject of future investigations.

## ACKNOWLEDGMENTS

The authors thank Drs A. Baartscheer and J.W.T Fiolet for the fruitful discussions and H.D. Beekman for the excellent technical assistance. This work was supported by a NWO grant (916.56.145) to Gudrun Antoons.

## REFERENCES

- Aker, S., Snabaitis, A. K., Konietzka, I., Van De Sand, A., Bongler, K., Avkiran, M., et al. (2004). Inhibition of the  $\text{Na}^+/\text{H}^+$  exchanger attenuates the deterioration of ventricular function during pacing-induced heart failure in rabbits. *Cardiovasc. Res.* 63, 273–282. doi: 10.1016/j.cardiores.2004.04.014
- Andersen, G. O., Oie, E., Vinge, L. E., Yndestad, A., Attramadal, H., Skomedal, T., et al. (2006). Increased expression and function of the myocardial Na-K-2Cl cotransporter in failing rat hearts. *Basic Res. Cardiol.* 101, 471–478. doi: 10.1007/s00395-006-0604-5
- Antoons, G., Oros, A., Beekman, H., Houtman, M., Engelen, M., Belardinelli, L., et al. (2008). Inhibition of late Na-current by ranolazine reduces Torsade de Pointes arrhythmias in the dog with chronic atrio-ventricular block. *Heart Rhythm Abstr.* 5, S115.
- Antoons, G., Oros, A., Bito, V., Sipido, K. R., and Vos, M. A. (2007). Cellular basis for triggered ventricular arrhythmias that occur in the setting of compensated hypertrophy and heart failure: considerations for diagnosis and treatment. *J. Electrocardiol.* 40, S8–S14. doi: 10.1016/j.jelectrocard.2007.05.022
- Baartscheer, A. (2006). Chronic inhibition of  $\text{Na}^+/\text{H}^+$ -exchanger in the heart. *Curr. Vasc. Pharmacol.* 4, 23–29. doi: 10.2174/157016106775203117
- Baartscheer, A., and van Borren, M. M. G. J. (2008). Sodium ion transporters as new therapeutic targets in heart failure. *Cardiovasc. Hematol. Agents Med. Chem.* 6, 229–236. doi: 10.2174/187152508785909546
- Baartscheer, A., Hardziyenka, M., Schumacher, C. A., Belterman, C. N., van Borren, M. M. G. J., Verkerk, A. O., et al. (2008). Chronic inhibition of the  $\text{Na}^+/\text{H}^+$  exchanger causes regression of hypertrophy, heart failure, and ionic and electrophysiological remodeling. *Br. J. Pharmacol.* 154, 1266–1275. doi: 10.1038/bjp.2008.189
- Baartscheer, A., Schumacher, C. A., van Borren, M. M. G. J., Belterman, C. N., Coronel, R., Opthof, T., et al. (2005). Chronic inhibition of  $\text{Na}^+/\text{H}^+$ -exchanger attenuates cardiac hypertrophy and prevents cellular remodeling in heart failure. *Cardiovasc. Res.* 65, 83–92. doi: 10.1016/j.cardiores.2004.09.024
- Baartscheer, A., Schumacher, C. A., van Borren, M. M. G. J., Belterman, C. N., Coronel, R., and Fiolet, J. W. (2003). Increased  $\text{Na}^+/\text{H}^+$ -exchange activity is the cause of increased  $[\text{Na}^+]_i$  and underlies disturbed calcium handling in the rabbit pressure and volume overload heart failure model. *Cardiovasc. Res.* 57, 1015–1024. doi: 10.1016/S0008-6363(02)00809-X
- Bers, D. M., Despa, S., and Bossuyt, J. (2006). Regulation of  $\text{Ca}^{2+}$  and  $\text{Na}^+$  in normal and failing cardiac myocytes. *Ann. N.Y. Acad. Sci.* 1080, 165–77. doi: 10.1196/annals.1380.015
- Bikkina, M., Larson, M. G., and Levy, D. (1993). Asymptomatic ventricular arrhythmias and mortality risk in subjects with left ventricular hypertrophy. *J. Am. Coll. Cardiol.* 22, 1111–1116. doi: 10.1016/0735-1097(93)90424-Y
- Camilion de Hurtado, M. C., Portiansky, E. L., Perez, N. G., Rebolledo, O. R., and Cingolani, H. E. (2002). Regression of cardiomyocyte hypertrophy in SHR following chronic inhibition of the  $\text{Na}^+/\text{H}^+$  exchanger. *Cardiovasc. Res.* 53, 862–868. doi: 10.1016/S0008-6363(01)00544-2
- Chen, L., Gan, X. T., Haist, J. V., Feng, Q., Lu, X., Chakrabarti, S., et al. (2001). Attenuation of compensatory right ventricular hypertrophy and heart failure following monocrotaline-induced pulmonary vascular injury by the  $\text{Na}^+/\text{H}^+$  exchange inhibitor cariporide. *J. Pharmacol. Exp. Ther.* 298, 469–476.
- Chiappe de Cingolani, G., Morgan, P., Mundina-Weilenmann, C., Casey, J., Fujinaga, J., Camilion de Hurtado, M., et al. (2001). Hyperactivity and altered mRNA isoform expression of the  $\text{Cl}^-/\text{HCO}_3^-$  anion-exchanger in the hypertrophied myocardium. *Cardiovasc. Res.* 51, 71–79. doi: 10.1016/S0008-6363(01)00276-0
- Cingolani, H. E., Perez, N. G., Aiello, E. A., Ennis, I. L., Garcarena, C. D., Villa-Abrille, M. C., et al. (2008). Early signals after stretch leading to cardiac hypertrophy. Key role of NHE-1. *Front. Biosci.* 13, 7096–7114. doi: 10.2741/3213
- Cingolani, H. E., Rebolledo, O. R., Portiansky, E. L., Perez, N. G., and Camilion de Hurtado, M. C. (2003). Regression of hypertensive myocardial fibrosis by  $\text{Na}^+/\text{H}^+$  exchange inhibition. *Hypertension* 41, 373–377. doi: 10.1161/01.HYP.0000051502.93374.1C
- Coccaro, E., Mraiche, F., Malo, M., Vandertol-Vanier, H., Bullis, B., Robertson, M., et al. (2007). Expression and characterization of the  $\text{Na}^+/\text{H}^+$  exchanger in the mammalian myocardium. *Mol. Cell. Biochem.* 302, 145–155. doi: 10.1007/s11010-007-9436-3
- Darmellah, A., Baetz, D., Prunier, E., Tamareille, S., Rucker-Martin, C., and Feuvray, D. (2007). Enhanced activity of the myocardial  $\text{Na}^+/\text{H}^+$  exchanger contributes to left ventricular hypertrophy in the Goto-Kakizaki rat model of type 2 diabetes: critical role of Akt. *Diabetologia* 50, 1335–1344. doi: 10.1007/s00125-007-0628-x
- Dart, C., and Vaughan-Jones, R. D. (1992).  $\text{Na}^+/\text{HCO}_3^-$  symport in the sheep cardiac Purkinje fibre. *J. Physiol.* 451, 365–385.
- Di Diego, J. M., Cordeiro, J. M., Goodrow, R. J., Fish, J. M., Zygmunt, A. C., Perez, G. J., et al. (2002). Ionic and cellular basis for the predominance of the Brugada syndrome phenotype in males. *Circulation* 106, 2004–2011. doi: 10.1161/01.CIR.0000032002.22105.7A
- Engelhardt, S., Hein, L., Keller, U., Klambt, K., and Lohse, M. J. (2002). Inhibition of  $\text{Na}^+/\text{H}^+$  exchange prevents hypertrophy, fibrosis, and heart failure in beta(1)-adrenergic receptor transgenic mice. *Circ. Res.* 90, 814–819. doi: 10.1161/01.RES.0000014966.97486.C0
- Ennis, I. L., Garcarena, C. D., Escudero, E. M. J., Perez, N. G., Dulce, R. A., Camilion de Hurtado, M. C., et al. (2007). Normalization of the calcineurin pathway underlies the regression of hypertensive hypertrophy induced by  $\text{Na}^+/\text{H}^+$  exchanger-1 (NHE-1) inhibition. *Can. J. Physiol. Pharmacol.* 85, 301–310. doi: 10.1139/y06-072
- Gerdes, A. M. (2002). Cardiac myocyte remodeling in hypertrophy and progression to failure. *J. Card. Fail.* 8, S264–S268. doi: 10.1054/jcaf.2002.129280
- Gray, R. P., McIntyre, H., Sheridan, D. S., and Fry, C. H. (2001). Intracellular sodium and contractile function in hypertrophied human and guinea-pig myocardium. *Pflügers Arch.* 442, 117–123. doi: 10.1007/s004240000512
- Gumina, R. J., Auchampach, J., Wang, R., Buerger, E., Eickmeier, C., Moore, J., et al. (2000).  $\text{Na}^+/\text{H}^+$  exchange inhibition-induced cardioprotection in dogs: effects on neutrophils versus cardiomyocytes. *Am. J. Physiol. Heart Circ. Physiol.* 279, H1563–H1570.
- Gumina, R. J., El Schultz, J., Moore, J., Beier, N., Schelling, P., and Gross, G. J. (2005). Cardioprotective-mimetics reduce myocardial infarct size in animals resistant to ischemic preconditioning. *Cardiovasc. Drugs Ther.* 19, 315–322. doi: 10.1007/s10557-005-3693-8
- Kilic, A., Velic, A., De Windt, L. J., Fabritz, L., Voss, M., Mitko, D., et al. (2005). Enhanced activity of the myocardial  $\text{Na}^+/\text{H}^+$  exchanger NHE-1 contributes to cardiac remodeling in atrial natriuretic peptide receptor-deficient mice. *Circulation* 112, 2307–2317. doi: 10.1161/CIRCULATIONAHA.105.542209
- Kondo, R. P., Dederko, D. A., Teutsch, C., Chrast, J., Catalucci, D., Chien, K. R., et al. (2006). Comparison of contraction and calcium handling between right and left ventricular myocytes from adult mouse heart: a role for repolarization waveform. *J. Physiol.* 571, 131–146. doi: 10.1113/jphysiol.2005.101428
- Kusumoto, K., Haist, J. V., and Karmazyn, M. (2001).  $\text{Na}^+/\text{H}^+$  exchange inhibition reduces hypertrophy and heart failure after myocardial infarction in rats. *Am. J. Physiol. Heart Circ. Physiol.* 280, H738–H745.
- Lagadic-Gossmann, D., Buckler, K. J., and Vaughan-Jones, R. D. (1992). Role of bicarbonate in pH recovery from intracellular acidosis in the guinea-pig ventricular myocyte. *J. Physiol.* 458, 361–384.
- Le Prigent, K., Lagadic-Gossmann, D., Mongodin, E., and Feuvray, D. (1997).  $\text{HCO}_3^-$ -dependent alkalinizing transporter in adult rat ventricular myocytes: characterization and modulation. *Am. J. Physiol.* 273, H2596–H2603.
- Leem, C. H., Lagadic-Gossmann, D., and Vaughan-Jones, R. D. (1999). Characterization of intracellular pH regulation in the guinea-pig ventricular myocyte. *J. Physiol.* 517(Pt 1), 159–180. doi: 10.1111/j.1469-7793.1999.01592.x
- Leem, C. H., and Vaughan-Jones, R. D. (1998). Out-of-equilibrium pH transients in the guinea-pig ventricular myocyte. *J. Physiol.* 509(Pt 2), 471–485. doi: 10.1111/j.1469-7793.1998.471bn.x



- Nakamura, T. Y., Iwata, Y., Arai, Y., Komamura, K., and Wakabayashi, S. (2008). Activation of  $\text{Na}^+/\text{H}^+$  exchanger 1 is sufficient to generate  $\text{Ca}^{2+}$  signals that induce cardiac hypertrophy and heart failure. *Circ. Res.* 103, 891–899. doi: 10.1161/CIRCRESAHA.108.175141
- Oh, K. S., Seo, H. W., Yi, K. Y., Lee, S., Yoo, S. E., and Lee, B. H. (2007). Effects of KR-33028, a novel  $\text{Na}^+/\text{H}^+$  exchanger-1 inhibitor, on ischemia and reperfusion-induced myocardial infarction in rats and dogs. *Fundam. Clin. Pharmacol.* 21, 255–263. doi: 10.1111/j.1472-8206.2007.00491.x
- Oikarinen, L., Nieminen, M. S., Viitasalo, M., Toivonen, L., Wachtell, K., Papademetriou, V., et al. (2001). Relation of QT interval and QT dispersion to echocardiographic left ventricular hypertrophy and geometric pattern in hypertensive patients. The LIFE study. The Losartan Intervention For Endpoint Reduction. *J. Hypertens.* 19, 1883–1891. doi: 10.1097/00004872-200110000-00025
- Pogwizd, S. M., Sipido, K. R., Verdonck, F., and Bers, D. M. (2003). Intracellular Na in animal models of hypertrophy and heart failure: contractile function and arrhythmogenesis. *Cardiovasc. Res.* 57, 887–896. doi: 10.1016/S0008-6363(02)00735-6
- Sandmann, S., Yu, M., Kaschina, E., Blume, A., Bouzinova, E., Aalkjaer, C., et al. (2001). Differential effects of angiotensin AT1 and AT2 receptors on the expression, translation and function of the  $\text{Na}^+/\text{H}^+$  exchanger and  $\text{Na}^+/\text{HCO}_3^-$  symporter in the rat heart after myocardial infarction. *J. Am. Coll. Cardiol.* 37, 2154–2165. doi: 10.1016/S0735-1097(01)01287-6
- Satoh, H., Delbridge, L. M., Blatter, L. A., and Bers, D. M. (1996). Surface:volume relationship in cardiac myocytes studied with confocal microscopy and membrane capacitance measurements: species-dependence and developmental effects. *Biophys. J.* 70, 1494–1504. doi: 10.1016/S0006-3495(96)79711-4
- Schoenmakers, M., Ramakers, C., van Opstal, J. M., Leunissen, J. D., Londono, C., and Vos, M. A. (2003). Asynchronous development of electrical remodeling and cardiac hypertrophy in the complete AV block dog. *Cardiovasc. Res.* 59, 351–359. doi: 10.1016/S0008-6363(03)00430-9
- Sipido, K. R., Volders, P. G., de Groot, S. H., Verdonck, F., Van de Werf, F., Wellens, H. J., et al. (2000). Enhanced  $\text{Ca}^{2+}$  release and Na/Ca exchange activity in hypertrophied canine ventricular myocytes: potential link between contractile adaptation and arrhythmogenesis. *Circulation* 102, 2137–2144. doi: 10.1161/01.CIR.102.17.2137
- Thomsen, M. B., Verduyn, S. C., Stengl, M., Beekman, J. D., de Pater, G., van Opstal, J., et al. (2004). Increased short-term variability of repolarization predicts d-sotalol-induced torsades de pointes in dogs. *Circulation* 110, 2453–2459. doi: 10.1161/01.CIR.0000145162.64183.C8
- Tomaselli, G. F., and Marban, E. (1999). Electrophysiological remodeling in hypertrophy and heart failure. *Cardiovasc. Res.* 42, 270–283. doi: 10.1016/S0008-6363(99)00017-6
- van Borren, M. M. G. J., Baartscheer, A., Wilders, R., and Ravesloot, J. H. (2004). NHE-1 and NBC during pseudo-ischemia/reperfusion in rabbit ventricular myocytes. *J. Mol. Cell. Cardiol.* 37, 567–577. doi: 10.1016/j.yjmcc.2004.05.017
- van Borren, M. M. G. J., Zegers, J., Baartscheer, A., and Ravesloot, J. H. (2006). Contribution of NHE-1 to cell length shortening of normal and failing rabbit cardiac myocytes. *J. Mol. Cell. Cardiol.* 41, 706–715. doi: 10.1016/j.yjmcc.2006.07.001
- van Opstal, J. M., Verduyn, S. C., Leunissen, H. D., de Groot, S. H., Wellens, H. J., and Vos, M. A. (2001). Electrophysiological parameters indicative of sudden cardiac death in the dog with chronic complete AV-block. *Cardiovasc. Res.* 50, 354–361. doi: 10.1016/S0008-6363(01)00226-7
- Verdonck, F., Volders, P. G., Vos, M. A., and Sipido, K. R. (2003). Increased  $\text{Na}^+$  concentration and altered Na/K pump activity in hypertrophied canine ventricular cells. *Cardiovasc. Res.* 57, 1035–1043. doi: 10.1016/S0008-6363(02)00734-4
- Verduyn, S. C., Vos, M. A., van der Zande, J., Kulcsar, A., and Wellens, H. J. (1997). Further observations to elucidate the role of interventricular dispersion of repolarization and early afterdepolarizations in the genesis of acquired torsade de pointes arrhythmias: a comparison between almokalant and d-sotalol using the dog as its own control. *J. Am. Coll. Cardiol.* 30, 1575–1584. doi: 10.1016/S0735-1097(97)00333-1
- Volders, P. G., Sipido, K. R., Carmeliet, E., Spatjens, R. L., Wellens, H. J., and Vos, M. A. (1999). Repolarizing  $\text{K}^+$  currents ITO1 and IKs are larger in right than left canine ventricular midmyocardium. *Circulation* 99, 206–210. doi: 10.1161/01.CIR.99.2.206
- Vos, M. A., de Groot, S. H., Verduyn, S. C., van der Zande, J., Leunissen, H. D., Cleutjens, J. P., et al. (1998). Enhanced susceptibility for acquired torsade de pointes arrhythmias in the dog with chronic, complete AV block is related to cardiac hypertrophy and electrical remodeling. *Circulation* 98, 1125–1135. doi: 10.1161/01.CIR.98.11.1125
- Yamamoto, T., Shirayama, T., Sakatani, T., Takahashi, T., Tanaka, H., Takamatsu, T., et al. (2007). Enhanced activity of ventricular  $\text{Na}^+/\text{HCO}_3^-$  cotransport in pressure overload hypertrophy. *Am. J. Physiol. Heart Circ. Physiol.* 293, H1254–H1264. doi: 10.1152/ajpheart.00964.2006
- Yamamoto, T., Swietach, P., Rossini, A., Loh, S. H., Vaughan-Jones, R. D., and Spitzer, K. W. (2005). Functional diversity of electrogenic  $\text{Na}^+/\text{HCO}_3^-$  cotransport in ventricular myocytes from rat, rabbit and guinea pig. *J. Physiol.* 562, 455–475. doi: 10.1113/jphysiol.2004.071068
- Yokoyama, H., Gunasegaram, S., Harding, S. E., and Avkiran, M. (2000). Sarcolemmal  $\text{Na}^+/\text{H}^+$  exchanger activity and expression in human ventricular myocardium. *J. Am. Coll. Cardiol.* 36, 534–540. doi: 10.1016/S0735-1097(00)00730-0

**Conflict of Interest Statement:** The authors declare that the research was conducted in the absence of any commercial or financial relationships that could be construed as a potential conflict of interest.

Received: 01 August 2013; paper pending published: 26 August 2013; accepted: 16 October 2013; published online: 26 November 2013.

Citation: van Borren MMGJ, Vos MA, Houtman MJC, Antoons G and Ravesloot JH (2013) Increased sarcolemmal  $\text{Na}^+/\text{H}^+$  exchange activity in hypertrophied myocytes from dogs with chronic atrioventricular block. *Front. Physiol.* 4:322. doi: 10.3389/fphys.2013.00322

This article was submitted to Membrane Physiology and Membrane Biophysics, a section of the journal *Frontiers in Physiology*.

Copyright © 2013 van Borren, Vos, Houtman, Antoons and Ravesloot. This is an open-access article distributed under the terms of the Creative Commons Attribution License (CC BY). The use, distribution or reproduction in other forums is permitted, provided the original author(s) or licensor are credited and that the original publication in this journal is cited, in accordance with accepted academic practice. No use, distribution or reproduction is permitted which does not comply with these terms.